The Astrophysical Journal Letters, 981:L21 (3pp), 2025 March 1 https://doi.org/10.3847/2041-8213/adb488

Erratum "Overestimation of Astrophysical Gamma-Ray Energies during Thunderstorms: Synergy of Galactic and Atmospheric Accelerators" (2024, ApJL, 975, L39)

A. Chilingarian and M. Zazyan
Yerevan Physics Institute, Alikhanian Brothers 2, Yerevan, AM0036, Armenia
Received 2025 January 24; published 2025 February 28

The authors apologize for the inconsistency between Tables 1 and 2 in the published Letter (A. Chilingarian & M. Zazyan 2024). The overestimation of high-energy gamma rays is influenced by the strength of the atmospheric electric field, E_z, and the height of the electric field above the surface, H. The extensive air shower (EAS) electrons, which multiply within the thundercloud, quickly attenuate after exiting the electric field. Therefore, the height of the electric field above the surface is a crucial factor affecting the number of electrons that reach the surface detector used for estimating the energy of the primary gamma rays. We calculated various values of H, determined the multiplication of electrons, and predicted the overestimation of energy for different combinations of E_z and H values. In the published Letter, we present tables of the multiplied number of electrons for just one value of H (Table 1) but mistakenly included the corresponding table of overestimation for a different value of H (Table 2). In this Erratum, we provide the corrected calculations for several H values and illustrate the relationship between energy overestimation and the height of the electric field above the surface detector.

1. Introduction

Electric fields induced by strong thunderstorms transfer energy to free electrons, accelerating them and, under specific conditions, forming electron–photon avalanches. In 1992, Gurevich, Milikh, and Roussel-Dupré defined the conditions for significant electron multiplication for each energetic seed electron introduced into the strong-field region (A. V. Gurevich et al. 1992). This mechanism, now known as the relativistic runaway electron avalanche (RREA; L. P. Babich et al. 2001; V. V. Alexeenko et al. 2002), multiplies seed electrons up to 100 times, extending their energy spectrum to 100 MeV. A numerical method to solve the relativistic Boltzmann equation for runaway electron beams (E. M. D. Symbalisty et al. 1998) aids in estimating the threshold (critical) field (L. P. Babich et al. 2001; J. R. Dwyer 2003) needed to initiate RREA. At standard temperature and pressure in dry air at sea level, $E_{\rm th} \approx 2.80 \times n$ kV cm^{-1}, with air density (n) relative to sea level. The strength of the threshold (critical) field is 20%–30% higher than this field because seed electrons do not always travel along the electric field lines; their trajectories deviate due to Coulomb scattering with atomic nuclei and Møller scattering with atomic electrons. After leaving the strong electric field E_z, electrons lose energy through ionization in dense air. If E_z decreases below the critical value at $H = 200$ m, only a few electrons with energies above 30 MeV can reach the surface from an approximate height of 3000–4000 m (A. Chilingarian et al. 2023). Thus, both E_z and H must be considered when evaluating the expected overestimation of gamma-ray energy during strong thunderstorms.

2. Estimation of the Primary Gamma-Ray Energy after Propagation in the Strong Atmospheric Electric Field

The Cosmic Ray Simulations for Cascade (CORSIKA; D. D. Heck et al. 1998) provide the quantity, energy, coordinates, and angles of incidence of secondary leptons and hadrons at various atmospheric levels for incident primary particles with energies up to 1000 PeV. The latest CORSIKA versions include acceleration and multiplication processes that emerge when charged particles enter the atmospheric electric field (AEF), which can be introduced at different altitudes. In our simulations, primary gamma rays with fixed energies (1, 10, 50, and 100 TeV) enter the atmosphere vertically, and all secondary particles are tracked from their first interaction in the atmosphere to a height of 4410 m (the location of the LHAASO observatory). The AEF of 1.7–1.9 kV m^{-1} was 2 km in the atmosphere at 150, 100, 50, and 0 m above the ground. This way, we tested the influence of the AEF height on enhancing EAS particles. The electrons and gamma rays were tracked and recorded until their energies exceeded 3 MeV. Tables 1 and 2 present CORSIKA calculations for two heights ($H = 0$ and 100 m), assuming several primary gamma-ray energies and strengths of AEFs. In the upper part of the tables, we put the number of electrons and positrons ($N_{\rm e}$) reaching the detector, and in the lower part, the estimated energy ($E_{\rm est}$) obtained by the linear fit, using CORSIKA simulation at fair weather ($E_z = 0$), second column of upper tables:

$$\text{Log } E_{\rm est} = 0.8364 \text{ Log } N_{\rm e} - 2.0842. \quad (1)$$

The $N_{\rm e}$ values for simulations with $H = 100$ m are significantly (4–7 times) lower than for $H = 0$ m (E_z continued until surface) due to attenuation of the electron flux in the dense atmosphere. Correspondingly, energies obtained by Equation (1) were overestimated by 6–12 times dependent on E_z.

Figures 1(a)–(d) show the electron flux surges after propagating through AEFs of varying strengths. The increase in electrons is significantly greater for the small H values when the electric field is close to the Earth's surface.

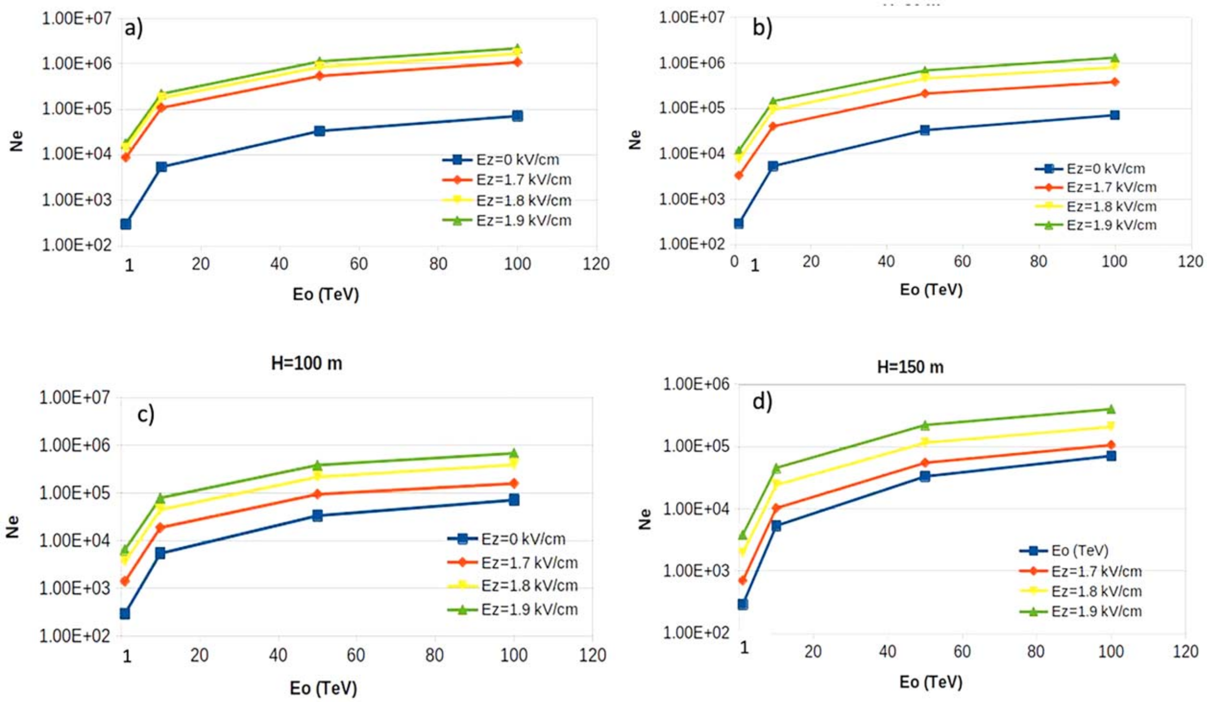

Figure 1. The enhancement of EAS electrons after their propagation in various AEFs (E_z), which terminated at different heights H above the surface.

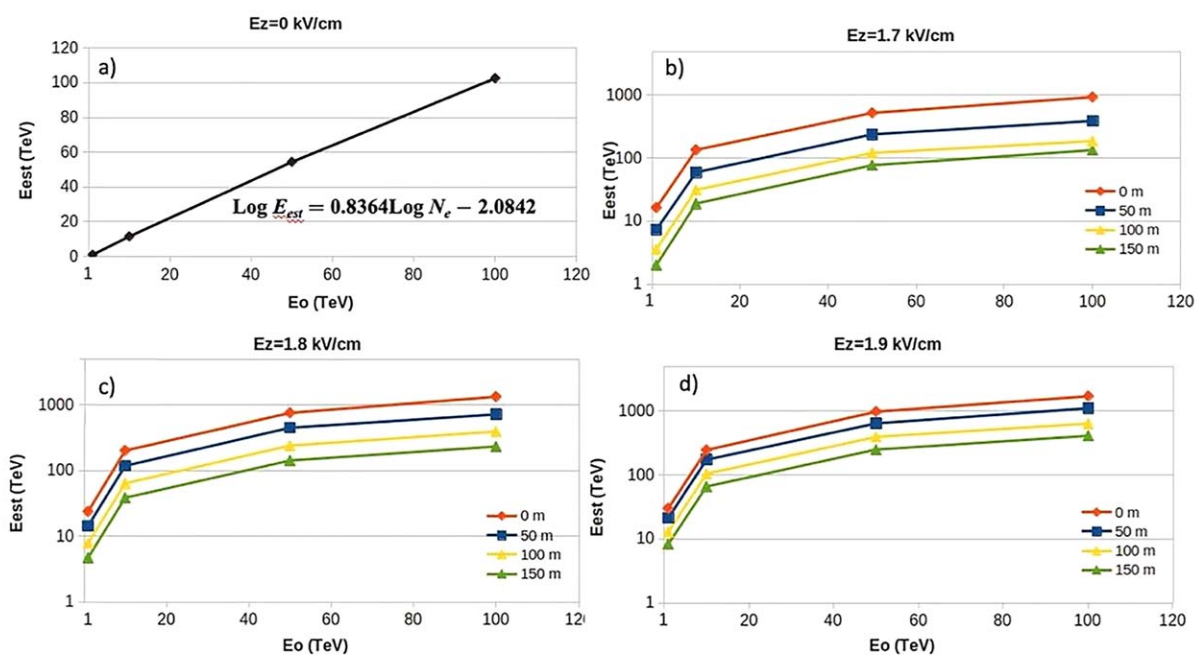

Figure 2. (a) Illustration of fitting procedure; (b)–(d) Relationship between "true" and estimated primary gamma-ray energies for different AEFs and H values.

In Figure 2(a), we illustrate the fitting procedure that leads to Equation (1). In Figures 2(b)–(d), we show the relationship between the primary energies of the simulations, which range from 1 to 100 TeV, and the estimates derived from Equation (1). As E_z increases, the overestimation becomes more significant, exceeding tenfold for 100 TeV primaries at all tested electric field strengths. This overestimation is twofold to sixfold when the accelerating electric field terminates 100 m above the surface. For lower primary energies, the overestimation is even greater.

3. Conclusion

We present corrected tables (Tables 1 and 2) confirming the overestimation of the primary gamma-ray energy when the EAS propagates through a strong electric field. The results indicate that the overestimation depends on both the strength of the AEF and the height above the surface when the accelerated electric field terminates.

Table 1
The Burst of Electrons by RREA and Primary Gamma-Ray Energy Estimates

E_o (TeV)	N_e, $E_z = 0$ kV cm^{-1}	N_e, $E_z = 1.7$ kV cm^{-1}	N_e, $E_z = 1.8$ kV cm^{-1}	N_e, $E_z = 1.9$ kV cm^{-1}
1	295	8678	13,738	18,011
10	5415	108,611	177,165	220,795
50	33,606	546,862	858,476	1,143,322
100	71,784	1,091,520	1,695,682	2,223,885
E_o (TeV)	E_{est}, $E_z = 0$ kV cm^{-1}	E_{est}, $E_z = 1.7$ kV cm^{-1}	E_{est}, $E_z = 1.8$ kV cm^{-1}	E_{est}, $E_z = 1.9$ kV cm^{-1}
1	0.99	16.31	23.96	30.05
10	11.27	135.22	203.65	244.86
50	52.84	523.12	763.01	969.81
100	99.35	932.89	1348.84	1692.52

Note. The electric field extended to 4410 m ($H = 0$ m).

Table 2
The Burst of Electrons by RREA and Primary Gamma-Ray Energy Estimates

E_o (TeV)	N_e, $E_z = 0$ kV cm^{-1}	N_e, $E_z = 1.7$ kV cm^{-1}	N_e, $E_z = 1.8$ kV cm^{-1}	N_e, $E_z = 1.9$ kV cm^{-1}
1	295	1406	3630	6527
10	5415	18,871	44,927	79,502
50	33,606	94,792	218,197	387,809
100	71,784	159,392	393,315	686,878
E_o (TeV)	E_{est}, $E_z = 0$ kV cm^{-1}	E_{est}, $E_z = 1.7$ kV cm^{-1}	E_{est}, $E_z = 1.8$ kV cm^{-1}	E_{est}, $E_z = 1.9$ kV cm^{-1}
1	0.99	3.56	7.86	12.85
10	11.27	31.25	64.59	104.14
50	52.84	120.66	242.45	392.35
100	99.35	186.41	397.01	633.09

Note. The electric field extended to 4510 m ($H = 100$ m).

ORCID iDs

A. Chilingarian https://orcid.org/0000-0002-2018-9715

References

Alexeenko, V. V., Khaerdinov, N. S., Lidvansky, A. S., et al. 2002, PhLA, 301, 299
Babich, L. P., Donskoy, E. N., Kutsyk, I. M., & Kudryavtsev, A. Y. 2001, ITPS, 29, 430
Chilingarian, A., Hovsepyan, G., Aslanyan, D., et al. 2023, JGRD, 128, e2022JD037309
Chilingarian, A., & Zazyan, M. 2024, ApJL, 975, L39
Dwyer, J. R. 2003, GeoRL, 30, 2055
Gurevich, A. V., Milikh, G. M., & Roussel-Dupre, R. 1992, PhLA, 165, 463
Heck, D., Knapp, J., Capdevielle, J. N., Schatz, G., & Thouw, T. 1998, Report No. FZKA 6019, Forschungszentrum (Nuclear Research Center), Karlsruhe, https:www.ikp.kit.edu/corsika/70.php
Symbalisty, E. M. D., Roussel-Dupré, R. A., & Yukhimuk, V. A. 1998, ITPS, 26, 1575